

X-RAY EMISSION FROM THE PRE-PLANETARY NEBULA HENIZE 3-1475

RAGHVENDRA SAHAI¹, JOEL H. KASTNER², ADAM FRANK³, MARK MORRIS⁴, ERIC G. BLACKMAN³
 raghvendra.sahai@jpl.nasa.gov
 Draft version October 29, 2018

ABSTRACT

We report the first detection of X-ray emission in a pre-planetary nebula, Hen 3-1475. Pre-planetary nebulae are rare objects in the short transition stage between the Asymptotic Giant Branch and planetary nebula evolutionary phases, and Hen 3-1475, characterised by a remarkable S-shaped chain of optical knots, is one of the most noteworthy members of this class. Observations with the Advanced CCD Imaging Spectrometer (ACIS) onboard the Chandra X-Ray observatory show the presence of compact emission coincident with the brightest optical knot in this bipolar object, which is displaced from the central star by 2''7 along the polar axis. Model fits to the X-ray spectrum indicate an X-ray temperature and luminosity, respectively, of $(4.3 - 5.7) \times 10^6$ K and $(4 \pm 1.4) \times 10^{31}$ (D/5 kpc)² erg s⁻¹, respectively. Our 3σ upper limit on the luminosity of compact X-ray emission from the central star in Hen 3-1475 is $\sim 5 \times 10^{31}$ (D/5 kpc)² erg s⁻¹. The detection of X-rays in Hen 3-1475 is consistent with models in which fast collimated post-AGB outflows are crucial to the shaping of planetary nebulae; we discuss such models in the context of our observations.

Subject headings: ISM: jets and outflows – planetary nebulae: individual (Hen3-1475) – stars: AGB and post-AGB, stars: mass loss – circumstellar matter – X-rays: ISM

1. INTRODUCTION

Pre-Planetary nebulae (PPNs)⁵ – objects in transition between the Asymptotic Giant Branch and planetary nebula (PN) phases – hold the key to some of the most vexing problems in our understanding of these very late stages of stellar evolution for intermediate mass ($\sim 1 - 8M_{\odot}$) stars. Observationally, PNs show a dazzling variety of morphologies (e.g., Schwarz, Corradi, & Melnick 1992; Sahai & Trauger 1998), whereas AGB stars are surrounded by roughly spherical gas-dust envelopes due to dense, slow stellar winds ejected with rates up to $10^{-4}M_{\odot}$ yr⁻¹ (e.g. Neri et al. 1998). In the short transition period between the AGB and PN phases, these objects turn on very fast winds (with speeds of a few $\times 100$ to ~ 2000 km s⁻¹) which interact violently with the surrounding envelopes, and drastically modify their spatio-kinematic structures. The nature and origin of such outflows remains unknown, and their interaction with the ambient circumstellar material and the consequent changes in the kinematics and morphology of the circumstellar material are very poorly understood.

X-ray (0.1-10 keV) observations can probe the direct signature of the interaction of the fast and slow winds, i.e. the very hot (10^7 - 10^8 K) gas which should be produced in the shocked region. As a result, many searches for X-ray emission from PNs have been conducted beginning with the Einstein observatory (mid-1980s), followed by EXOSAT and ROSAT, and continue now with CXO and XMM-Newton. Prior to ROSAT, most X-rays in PNs were interpreted as coming from the hot ($1-2 \times 10^5$ K) central star; ROSAT data led to the identification of *diffuse* emission

from 7 PNs but several of these were erroneous (Kreysing et al. 1992, Guerrero, Chu & Gruendl 2000). With CXO and XMM, extended X-ray emission from PNs has been unambiguously imaged, and results have been reported for 5 objects (BD+30°3639, NGC7027, Mz 3: Kastner et al. 2000,2001,2003; NGC6543: Chu et al. 2001; NGC7009: Guerrero, Gruendl & Chu 2002). These studies clearly show the presence of extended bubbles of hot ($\sim 10^6$ K) gas, in qualitative agreement with our expectations from interacting-winds models.

X-ray observations of PPNs provide us with a unique opportunity to study magnetic fields, which may play an important role in shaping planetary nebulae (e.g. Balick & Frank 2002), indirectly (acting as the collimation agent of the fast outflows: Garcia-Segura 1997, Gardiner & Frank 2001) or directly (magneto-centrifugal launching of disk winds: Blackman, Frank and Welch 2000). Unlike most PNs, the central stars of PPNs are too cold to provide blackbody X-ray emission, thus detection of a compact central source of X-rays in a PPN could provide direct evidence for the presence of a strong stellar magnetic field. E.g., by analogy with the solar dynamo, new AGB-stellar-dynamo modelling (Blackman et al. 2001) predicts a strong field (of few $\times 10^4$ G) near the base of the star's convection zone with a 0.2 yr decay half-cycle (11 yrs for the Sun); dissipation of this field should result in a non-thermal X-ray luminosity of $\sim 10^{32}$ erg s⁻¹ from the central stars in very young PPNs.

However, no systematic search for X-ray emission from PPNs has been carried out to-date, because until very recently, it was believed that the wind-wind interaction re-

¹ Jet Propulsion Laboratory, MS 183-900, Caltech, Pasadena, CA 91109

² Chester F. Carlson Center for Imaging Science, Rochester Institute of Technology, Rochester, NY 14623

³ Dept. of Physics & Astronomy, University of Rochester, Rochester, NY 14627

⁴ Division of Astronomy & Astrophysics, UCLA, Los Angeles, CA 90095

⁵ We prefer this phrase to “proto-planetary” nebula, which although in more common use for these objects, is also potentially misleading because the same term is used by the young stellar object community

sponsible for shaping PNs occurred during the PN phase (through the interaction of a fast radiatively-driven spherical wind from the central hot white dwarf with an equatorially-dense wind from the AGB phase). In this *Letter*, we report our discovery of X-ray emission from the well-studied PPN Hen 3-1475. This remarkable S-shaped object was selected as the prime target in our search for X-ray emission from PPNs because it shows the presence of an ultra-fast outflow ($\sim 2300 \text{ km s}^{-1}$) (Sánchez Contreras & Sahai 2001), and bright optical knots of emission from shocked gas (Borkowski & Harrington 2001; Riera et al. 2003).

2. OBSERVATIONS & RESULTS

We observed Hen 3-1475 with the Chandra X-Ray Observatory (CXO) for 49.7 ks on 2002 July 15, using the back-illuminated CCD S3 of the Advanced CCD Imaging Spectrometer (ACIS). The CXO/ACIS combination is sensitive over the energy range 0.3-10 keV. ACIS has a pixel size of $0.49''$, very similar to the width of the point spread function (PSF) of the Chandra mirrors. The data, consisting of individual CCD X-ray and particle events, were subject to standard processing by Chandra X-ray Center pipeline software (CIAO⁶, version 2.0), which determines the distribution of photon-generated charge within a 3×3 CCD pixel box centered on the event position, flags events likely due to particles, and computes the celestial positions and nominal energies of incident X-rays. In order to optimize image resolution, the event charge distributions were used, along with the telescope pointing history and nominal photon energies, to calculate a subpixel position for each X-ray (Li et al. 2003).

The CXO/ACIS-S3 image of Hen 3-1475 (Fig. 1) shows the presence of compact emission coincident with the brightest optical knot in this object (NW1a in Fig. 1, (Riera et al. 2003)), as seen in a Hubble Space Telescope (HST) image taken with the Wide Field & Planetary Camera 2 (WFPC2) in the [OIII] (F502N) filter. The relative registration of the optical and X-ray images has been established as follows: (1) the USNO-B.1 catalog was used to determine the optical position of the central star in Hen 3-1475 ($\alpha = 17^{\text{h}}45^{\text{m}}14^{\text{s}}.186$, $\delta = -17^{\circ}56'46''.23$, J2000), and (2) the absolute CXO astrometry was used for the X-ray data, which locates the central peak of the X-ray emission at $\alpha = 17^{\text{h}}45^{\text{m}}14^{\text{s}}.05$, $\delta = -17^{\circ}56'44''.81$, i.e. offset by $2''.0$ W, $1''.4$ N from the central star. The peak of the optical (NW1a) knot is located $1''.95$ W, $1''.9$ N, of the central star. Taking into account (a) the size of the optical knot (about $0''.7$ along the nebular axis), (b) the sizes of the CXO PSF and the ACIS-S3 pixel size (about $0''.5$), and (c) the uncertainty in the CXO absolute astrometry ($\sim 0''.6$), we believe that the X-ray emission and the optical knot are co-spatial, and thus physically associated. The probability of chance association of a background X-ray source with the knot is very small, considering that the optical knot covers only $\sim 10^{-5}$ of a region of $\sim 2 \text{ arcmin}^2$ around the source in which there are only a few (< 5) X-ray sources.

The spectrum of the X-ray emitting knot is fairly soft, with almost all the flux confined to the 0.4–1.6 keV energy band (a total of 63 ± 8 counts, corresponding to a background-subtracted count rate of $1.5 \times 10^{-3} \text{ cps}$) (Fig.

2). The spectrum was extracted using CIAO tools (ver. 2.3), a 5 pixel ($2''.5$) radius circular source region centered on the X-ray knot and a somewhat larger circular background region centered $\sim 20''$ west of the source. The spectrum peaks around 0.85 keV, similar to the ACIS-S spectrum of Mz 3 (Kastner et al. 2003). In contrast, two background sources in the vicinity of Hen 3-1475 have significantly harder spectra.

We have fitted the X-ray spectrum with a model consisting of VMEKAL thermal emission plus “standard ISM” intervening absorption (Morrison & McCammon 1983); a value of $A_V=2$ is assumed for the latter (Riera et al. 1995). Assuming solar abundances, the values of the plasma temperature kT and the source flux were varied; the best-fit, assuming a 20% uncertainty in A_V , gives a temperature, $T_x = (4.3 - 5.7) \times 10^6 \text{ K}$, and an “unabsorbed” X-ray flux, $F_x = (0.87 - 1.8) \times 10^{-14} \text{ erg cm}^{-2} \text{ s}^{-1}$, where the lower (upper) limit for F_x corresponds to the upper (lower) limit for T_x .

Although the above model provides a reasonable fit to the observed spectrum, the latter shows an excess (relative to the model) around 0.65 keV. Since oxygen (O VIII) can contribute to this feature via line emission at 19\AA , we have tried models in which the O abundance is allowed to vary freely. We find that there is a hint of O enhancement in the X-ray-emitting gas, but the signal-to-noise ratio is insufficient to determine abundances. Unless, e.g., Fe is severely depleted in Hen 3-1475 (as may be the case for BD+30°3639; Maness et al. 2003), the best-fit value of T_x obtained from the solar abundance model is likely to be reasonably accurate. The X-ray flux (F_x) determination is fairly robust even if heavy metals are severely depleted.

Our derived F_x gives an intrinsic X-ray luminosity for Hen 3-1475 of $L_x = (4 \pm 1.4) \times 10^{31} \text{ (D/5 kpc)}^2 \text{ erg s}^{-1}$. Using our model volume emission measure, $\text{EM} \sim 10^{54} \text{ cm}^{-3}$, and the electron density for the NW knot ($\sim 3000 \text{ cm}^{-3}$) from Riera et al. (1995), we find that the X-ray emitting volume is $V_x \sim 10^{47} \text{ cm}^3$, which is a small fraction of the optically emitting volume ($V_{\text{opt}} \sim 3 \times 10^{48} \text{ cm}^3$), as derived from the knot size ($\sim 0''.2$) in the [OIII] image.

It is not surprising that X-ray emission is detected only from the NW1a knot, since this feature is also the brightest and highest-excitation optical jet feature, by far, as seen in the [OIII] $\lambda 5007$ image (Fig. 1). For example, the integrated [OIII] flux and the [OIII]/[NII] emission-line ratio of knot NW1a, are larger by factors 3.5 and $\gtrsim 2$, respectively, than the corresponding values for its point-symmetric counterpart (knot SE1a). The 1.4 mag of differential extinction between the knots ($A_V=3.4$ for SE1 knots, Riera et al. (1995)) reduces the X-ray flux of the SE1a knot by a factor 6.5 over the NW1a knot, insufficient to make it undetectable in our data. Thus, the difference in the X-ray emission (and optical emission) between knot NW1a and its SE counterpart probably results from a combination of differences in extinction and excitation.

We do not detect a compact X-ray source towards the central star in Hen 3-1475; a conservative upper limit (3σ) on the “unabsorbed” X-ray flux and intrinsic X-ray luminosity, respectively, of such a source is $F_c \sim 1.7 \times 10^{-14} \text{ erg cm}^{-2} \text{ s}^{-1}$ and $L_c \sim 5 \times 10^{31} \text{ (D/5 kpc)}^2 \text{ erg s}^{-1}$, using a temperature similar to that of the nebular source, and

⁶ <http://cxc.harvard.edu/ciao/>

$A_V = 3.4$, the value used Riera et al. (1995) for the central source in Hen 3-1475. Since the extinction towards the center could be higher, and the distance to Hen 3-1475 is rather uncertain, our upper limit is not inconsistent with the value predicted by Blackman et al. (2001) ($\sim 10^{32}$ ergs $^{-1}$) based on their solar-dynamo analog for producing magnetic fields in the central stars of PPN.

3. DISCUSSION

Recent HST studies of the morphology of young PNs and PPNs strongly support a model in which fast collimated outflows begin to modify the circumstellar environment during the PPN phase and/or even earlier, during the very late AGB phase (Sahai & Trauger 1998). Our discovery of nebular 0.4-1.6 keV X-ray emission from Hen 3-1475 dramatically confirms the operation of the resulting violent post-AGB wind/ AGB wind interaction process. The simultaneous presence of both X-ray and optical emission in the NW1a knot supports the idea that the knots are strongly-cooling regions of shocked gas with very strong temperature gradients. The S-shaped distribution of the fast-moving knots in this object indicates that the fast post-AGB wind consists of an episodic jet-like outflow whose axis has precessed with time (precession angle $<10^\circ$ and a period ~ 1500 years, Riera et al. (1995)). This scenario is supported by the theoretical result that a jet with a quasi-periodic variability and slow precession fragments into clumps which behave like “interstellar bullets” (Raga & Biro 1993).

Alternatively, the jet may intrinsically consist of a series of hypersonic bullets ejected by processes close to the surface of the star. Matt et al. (2004) have shown how the development of toroidal fields in a recently exposed PPN core could lead to an impulsive deposition of flow energy into a collimated system. Whatever their origin, recent work by Poludnenko, Frank, & Mitran (2004) has shown that hypersonic bullets are capable of recovering key aspects of many PPN flows. The temperatures deduced from the X-ray measurements could be achieved with shock velocities at the surface of the bullet of $v_s \approx \sqrt{(16kT_x/3m_h)} = 470 \text{ km s}^{-1}$. Note that although this speed is lower than that derived for the knots from observations (Borkowski & Harrington 2001; Riera et al. 2003), the relevant speed for comparison is that of the shock transmitted into the high density bullet, which will be lower than the bow shock speed. It is also possible that the bullet responsible for the X-ray knot will be moving into a medium which itself has been set into motion by the preceding bullet, leading to lower shock speeds.

If, however, the jet is a continuous flow, then the optical shape of the X-ray knot and its coincidence with the X-ray emission leads to another interesting possibility. The narrowing of the flow at the knot in Hen 3-1475 is not seen in other jet-producing environments and has been noted as a potential example of a “conical converging flow” in which material is inertially focused by the walls of an axisymmetric cavity to converge at a point where shocks redirect the material into a jet (Canto, Tenorio-Tagle, & R’ozyczka 1988; Frank, Balick, & Livio 1996). Recent laboratory experiments have shown such flows to be capable of producing remarkably stable jets (Lebedev et al. 2002). While the S-shaped symmetry evident in Hen 3-1475 makes pure hy-

drodynamic collimation unlikely, the presence of toroidal magnetic fields may produce conically converging flows in a similar manner which would also show X-rays at the convergence point. In fact, Hen 3-1475 is the first case of unambiguously shock-excited X-ray emitting gas to be detected by CXO that is unresolved (e.g., all of the PNs detected by CXO show resolved nebular X-ray emission). The various jet models for Hen 3-1475 described above need to be tested using detailed (magneto)hydrodynamic simulations to quantitatively fit the observed X-ray and optical (line) fluxes and spectra.

We are thankful for partial financial support for this work provided by NASA through its Long Term Space Astrophysics program (grant no. 399-30-61-00-00) for R.S. and M.M., as well as through Chandra Awards GO2-3029X (for R.S.) and GO2-3009X (for J.H.K./RIT) issued by the Chandra X-ray Observatory Center, which is operated by the Smithsonian Astrophysical Observatory on behalf of NASA under contract NAS8-39073.

REFERENCES

- Balick, B. & Frank, A. 2002, *ARAA*, 40, 439
- Borkowski, K. J. & Harrington, J. P. 2001, *ApJ*, 550, 778
- Blackman, E.G., Frank, A., Welch, C. 2000, *ApJ*, 546, 288
- Blackman, E.G., Frank, A., Markiel, J.A., Thomas, J.H., & Van Horn, H.M. 2001, *Nature*, 409, 485
- Canto J., Tenorio-Tagle G., & R'ozyczka M., 1988, *A&A*, 192, 287
- Chu, Y., Guerrero, M. A., Gruendl, R. A., Williams, R. M., & Kaler, J. B. 2001, *ApJ*, 553, L69
- Frank, A., Balick, B., & Livio, M., 1996, *ApJ*, 471, L53
- Garcia-Segura, G. 1997, *ApJ*, 489, L189
- Gardiner, T.A. & Frank, A. 2001, *ApJ*, 557, 250
- Guerrero, M.A., Chu, Y.-H., & Gruendl, R.A. 2000, *ApJ Suppl.Ser.* 129, 295
- Guerrero, M. A., Gruendl, R. A., & Chu, Y.-H. 2002, *A&A*, 387, L1
- Kastner, J.H., Soker, N., Vrtilik, S.D., & Dgani, R. 2000, *ApJ*, 545, L57
- Kastner, J.H., Vrtilik, S.D., & Soker, N., 2002, *ApJ*, 550, L189
- Kastner, J. H., Balick, B., Blackman, E. G., Frank, A., Soker, N., Vrtilik, S. D., & Li, J. 2003, *ApJ*, 591, L37
- Kreysing, H.C., Diesch, C., Zweigle, J., Staubert, R., & Grewing, M. 1993, *A&A*, 264, 623
- Lebedev, S.V., Chittenden, J.P., Beg, F.N., Bland, S.N., Ciardi, A., Ampleford, D., Hughes, S., Haines, M.G., Frank, A., Blackman, E.G. & Gardiner, T.A. 2002, *ApJ*, 564, 113
- Li, J., Kastner, J. H., Prigozhin, G. Y., & Schulz, N. S. 2003, *ApJ*, 590, 586
- Maness, H. L., Vrtilik, S. D., Kastner, J. H., & Soker, N. 2003, *ApJ*, 589, 439
- Matt, S., Blackman, E., Frank, A., 2004, in *Asymmetrical Planetary Nebulae III*, eds. M. Miexner, J. Kastner, N. Soker & B. Balick, (in press)
- Morrison, R. & McCammon, D. 1983, *ApJ*, 270, 119
- Neri, R., Kahane, C., Lucas, R., Bujarrabal, V., & Loup, C. 1998, *A&AS*, 130, 1
- Poludnenko, A., Frank, A., & Mitran, S., 2004, in *Asymmetrical Planetary Nebulae III*, eds. M. Miexner, J. Kastner, N. Soker & B. Balick, (in press)
- Raga, A. C. & Biro, S. 1993, *MNRAS*, 264, 758
- Riera, A., Garcia-Lario, P., Manchado, A., Pottasch, S. R., & Raga, A. C. 1995, *A&A*, 302, 137
- Riera, A., Garcia-Lario, P., Manchado, A., Bobrowsky, M., & Estalella, R. 2003, *A&A*, 401, 1039
- Sánchez Contreras, C. & Sahai, R. 2001, *ApJ*, 553, L173
- Sahai, R. & Trauger, J.T. 1998, *AJ*, 116, 1357
- Schwarz, H. E., Corradi, R. L. M., & Melnick, J. 1992, *A&AS*, 96, 23

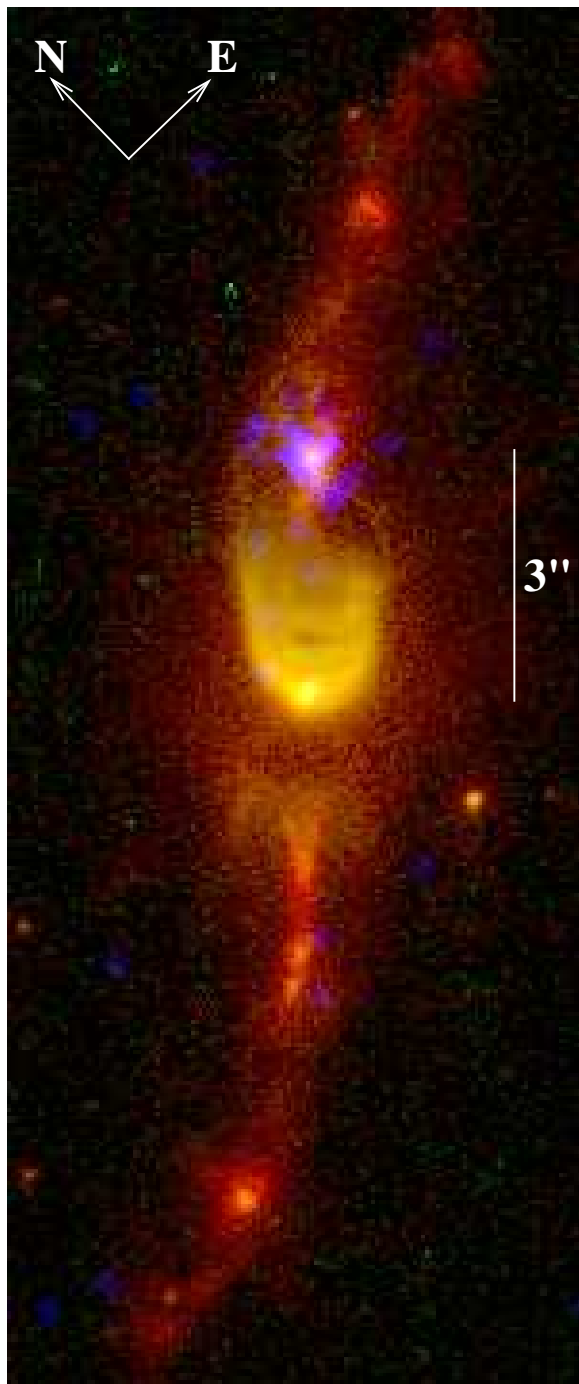


FIG. 1.— CXO/ACIS-S3 X-ray image (blue, linear stretch) overlaid on a composite HST image of Hen 3-1475 taken through the F507N ([OIII], green, log stretch) and F658N ([NII], red, log stretch) emission-line filters

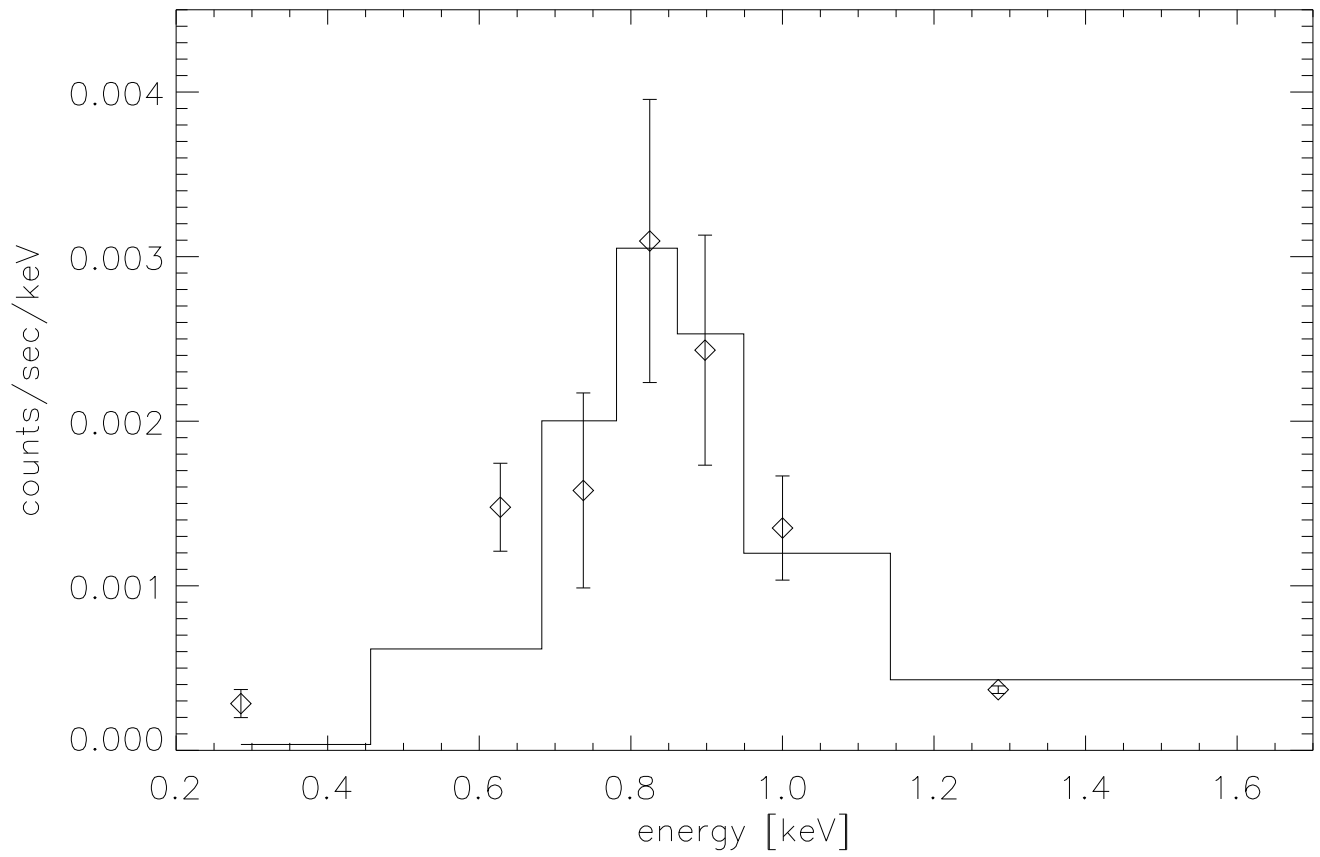


FIG. 2.— ACIS-S3 (background-subtracted) spectrum of Hen 3-1475, together with a best-fit VMEKAL plasma model with $T_x = 5 \times 10^6$ K